

**REVIEWS**

# The evolving biology of the proton-coupled folate transporter: New insights into regulation, structure, and mechanism

Zhanjun Hou<sup>1,2</sup>  | Aleem Gangjee<sup>3</sup> | Larry H. Matherly<sup>1,2,4</sup>

<sup>1</sup>Molecular Therapeutics Program, Barbara Ann Karmanos Cancer Institute, Detroit, Michigan, USA

<sup>2</sup>Department of Oncology, Wayne State University School of Medicine, Detroit, Michigan, USA

<sup>3</sup>Division of Medicinal Chemistry, Graduate School of Pharmaceutical Sciences, Duquesne University, Pittsburgh, Pennsylvania, USA

<sup>4</sup>Department of Pharmacology, Wayne State University School of Medicine, Detroit, Michigan, USA

**Correspondence**

Zhanjun Hou and Larry H. Matherly, Molecular Therapeutics Program, Barbara Ann Karmanos Cancer Institute, 421 East Canfield Street, Detroit, MI 48201, USA.  
Email: hou@karmanos.org and matherly@karmanos.org

**Funding information**

This work was supported by NIH/NCI grant R01 CA053535 (Z. Hou, L.H. Matherly), R01 CA250469 (L.H. Matherly, A. Gangjee), the Eunice and the Milton Ring Endowed Chair for Cancer Research (L.H. Matherly), and the Duquesne University Adrian Van

**Abstract**

The human proton-coupled folate transporter (PCFT; SLC46A1) or hPCFT was identified in 2006 as the principal folate transporter involved in the intestinal absorption of dietary folates. A rare autosomal recessive hereditary folate malabsorption syndrome is attributable to human SLC46A1 variants. The recognition that hPCFT was highly expressed in many tumors stimulated substantial interest in its potential for cytotoxic drug targeting, taking advantage of its high-level transport activity under acidic pH conditions that characterize many tumors and its modest expression in most normal tissues. To better understand the basis for variations in hPCFT levels between tissues including human tumors, studies have examined the transcriptional regulation of hPCFT including the roles of CpG hypermethylation and critical transcription factors and *cis* elements. Additional focus involved identifying key structural and functional determinants of hPCFT transport that, combined with homology models based on structural homologies to the bacterial transporters GlpT and LacY, have enabled new structural and mechanistic insights. Recently, cryo-electron microscopy structures of chicken PCFT in a substrate-free state and in complex with the antifolate pemetrexed were reported, providing further structural insights into determinants of (anti)folate recognition and the mechanism of pH-regulated (anti)folate transport by PCFT. Like many major facilitator proteins, hPCFT exists as a homo-oligomer, and evidence suggests that homo-oligomerization of hPCFT monomeric proteins may be important for its intracellular trafficking and/or transport function. Better

**Abbreviations:** AE1, anion exchanger 1; AP, activator protein; cPCFT, chicken PCFT; cryo-EM, cryo-electron microscopy; DDM, n-dodecyl- $\beta$ -D-maltoside; ENT1, equilibrative nucleoside transporter 1; FRET, fluorescence resonance energy transfer; GI, gastrointestinal; GlpT, glycerol-3-phosphate transporter; GLUT, glucose transporter; HA, hemagglutinin; HFM, hereditary folate malabsorption; HNF4 $\alpha$ , hepatocyte nuclear factor 4 $\alpha$ ; hPCFT, human PCFT; hRFC, human reduced folate carrier; KLF, Krüppel-like factor; LacS, lactose transport protein; LacY, lactose permease; LMNG, lauryl maltose neopentyl glycol; MFS, major facilitator superfamily; MTS-1-MTS, 1,1-methanediyl bismethanethiosulfonate; MTSEA, 2-aminoethyl methanethiosulfonate; NRF-1, nuclear respiratory factor-1; PCFT, proton-coupled folate transporter; PiPT, piriformospora indica phosphate transporter; PT523, N $^{\alpha}$ -(4-amino-4-deoxypteroyl)-N $^{\delta}$ -hemiphthaloyl-L-ornithine; SCAM, substituted cysteine accessibility methods; SERT, serotonin transporter; SLC, solute carrier; Sp1, stimulatory protein 1; TetA, tetracycline resistance protein; TMD, transmembrane domain; YY1, yin yang 1.

This is an open access article under the terms of the Creative Commons Attribution-NonCommercial-NoDerivs License, which permits use and distribution in any medium, provided the original work is properly cited, the use is non-commercial and no modifications or adaptations are made.

© 2022 The Authors. *The FASEB Journal* published by Wiley Periodicals LLC on behalf of Federation of American Societies for Experimental Biology.

Kaam Chair in Scholarly Excellence  
(A. Gangjee)

understanding of the structure, function and regulation of hPCFT should facilitate the rational development of new therapeutic strategies for conditions associated with folate deficiency, as well as cancer.

#### KEYWORDS

antifolate, major facilitator superfamily, membrane transporter, proton-coupled folate transporter

## 1 | INTRODUCTION

The proton-coupled folate transporter (PCFT; SLC46A1) was discovered in 2006 and was identified as the principal folate transporter involved in the intestinal absorption of dietary folates.<sup>1</sup> The recognition that human PCFT (hPCFT) is highly expressed in many tumors stimulated substantial interest in using hPCFT for cytotoxic drug targeting.<sup>2–8</sup> Reflecting the biological and therapeutic importance of PCFT, numerous studies have explored its transcriptional regulation, along with structural and functional determinants of PCFT transport. From structural homologies to the bacterial transporter GlpT, and bovine and rat GLUT5, homology models were developed for hPCFT,<sup>9–12</sup> enabling new mechanistic insights and experimentally testable hypotheses. Recently, cryo-electron microscopy (cryo-EM) structures of chicken PCFT (cPCFT) in a substrate-free state and in complex with the antifolate pemetrexed were reported.<sup>13</sup> Collectively, these results provide a structural basis for understanding antifolate recognition, including new insights into the pH-regulated mechanism of (anti)folate transport mediated by PCFT. This review summarizes the evolving biology of the PCFT as a prelude to the rational development of new therapeutic strategies for conditions associated with folate deficiency, as well as cancer.

## 2 | DISCOVERY AND TISSUE EXPRESSION OF PCFT

It was studies into the mechanism of facilitated transport of the new-generation antifolate, pemetrexed,<sup>14</sup> that eventually led to identification of a new facilitative folate transporter called PCFT.<sup>1</sup> Folates are absorbed across the brush-border membrane of the proximal intestine by PCFT, and PCFT is also essential to the transport of folates across the choroid plexus.<sup>1,15</sup> A defining characteristic of PCFT involves its substantial activity under acid conditions.<sup>16</sup> For the proximal small intestine where absorption of dietary folates occurs, the microenvironment pH is 5.8–6.0, reflecting the presence of sodium proton exchangers in the apical membrane.<sup>17–19</sup>

The human *SLC46A1* gene is located on chromosome 17q11.2 and includes five exons (Figure 1). Inherited

variants in the *SLC46A1* gene cause loss of expression or function of its encoded protein, resulting in a severely low levels of systemic and cerebral folates termed hereditary folate malabsorption (HFM).<sup>1,9,20,21</sup> HFM syndrome appears shortly after birth and is accompanied by anemia, gastrointestinal (GI) symptoms, immune deficiency, and neurologic manifestations.<sup>21</sup>

In addition to the upper GI and the choroid plexus, PCFT is expressed in other normal tissues, most notably the kidney, the sinusoidal membrane of the liver, the retinal pigment epithelium, spleen, and placenta.<sup>1,8,22–24</sup> hPCFT is highly expressed in many tumors (e.g., lung, ovarian, mesothelioma, and pancreatic cancers) and is expressed at very low levels in leukemias.<sup>3,5–8,25</sup> Transport by hPCFT is an important determinant of clinical response and resistance to pemetrexed, one of the two major drugs for malignant pleural mesothelioma and an important drug for treating nonsmall cell lung cancer.<sup>26,27</sup> In recent years, there has been growing interest in using hPCFT for targeting novel cytotoxic antifolates to tumors, taking advantage of its high-level activity at the acidic pH conditions associated with the microenvironment of many tumors and its unique structure-activity requirements from the ubiquitously expressed human reduced folate carrier (RFC; SLC19A1) or hRFC.<sup>2,8,28</sup>

To better understand the molecular basis for variations in hPCFT levels between tissues including human tumors, studies began examining the transcriptional regulation of hPCFT. The hPCFT promoter includes a large (~1 kb) CpG island which spans the transcriptional start site and can be hypermethylated, resulting in low hPCFT levels.<sup>25,29,30</sup> Treatment of low hPCFT-expressing cultured cells with 5-aza-2'-deoxycytidine restored hPCFT levels.<sup>25,29,30</sup> In mice fed a folate-deficient diet, PCFT transcript levels were increased ~13-fold in the proximal small intestine compared to mice fed a standard (folate-replete) diet<sup>31</sup>; however, it is unclear whether this increase in PCFT expression is associated with changes in promoter methylation or if other mechanisms are involved.

The hPCFT promoter (positions –3000 and +96 relative to the transcriptional start site at position +1)<sup>29</sup> includes cis elements for Sp1, AP1, AP2, NRF-1, KLF4, KLF15, HNF4 $\alpha$ , YY1, and vitamin D<sup>32–36</sup> (the human

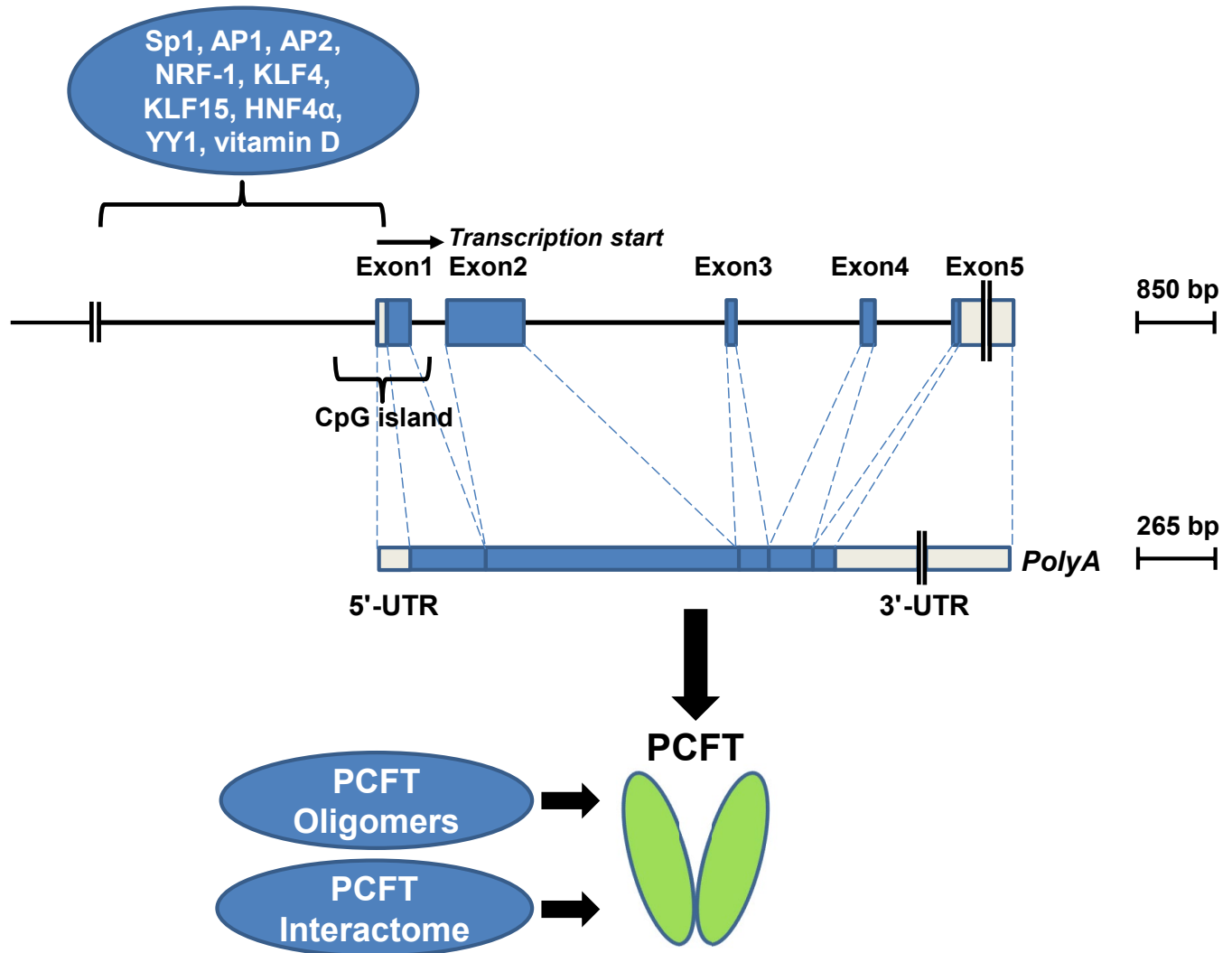


**FIGURE 1** Modes of hPCFT regulation. The genomic organization of the human *SLC46A1* gene (upper) and splicing of its transcript (lower) are depicted. For hPCFT, the ~1 kb CpG island and major transcription factor binding motifs are indicated from positions –3000 to +96, where the transcriptional start site is +1. Also depicted is the potential regulatory role associated with hPCFT homo-oligomerization. Although heterologous protein interactions have not yet been confirmed, protein interaction networks (“interactome”) could also play important roles in hPCFT regulation

*SLC46A1* gene structure including major transcription factors is depicted in Figure 1). The transcriptional basis for highly disparate expression of hPCFT between HepG2 (human hepatocellular carcinoma) (high) versus HT1080 (fibrosarcoma) (low) tumor cells was reflected the differential promoter binding of NRF-1, KLF15, and Sp1 proteins, paralleling intracellular levels of these transcription factors.<sup>36</sup> Sp1 phosphorylation was also suggested to regulate hPCFT transcription.<sup>36</sup>

### 3 | TRANSPORT PROPERTIES OF PCFT

PCFT is a proton symporter such that the proton gradient across the cell membrane drives the uphill transport of

folates into cells. PCFT operates most efficiently at acidic pH,<sup>16</sup> in striking contrast to the RFC, the major tissue folate transporter, which has a neutral pH optimum.<sup>37</sup> In tissues which express PCFT, RFC is invariably present. A dynamic interplay has been reported between these major folate transport systems that depends on transporter levels and extracellular pH.<sup>38</sup> In HEK293 (human embryonic kidney) cells, hPCFT transport is maximal at pH 4.5,<sup>39</sup> with significant activity up to pH 6.5.<sup>16</sup> As extracellular pH is further increased, hPCFT transport decreases precipitously. hPCFT substrates include 5-methyl tetrahydrofolate, 5-formyl tetrahydrofolate, and classic antifolates such as methotrexate and pemetrexed.<sup>1,8,16</sup> Transport is specific for (6S)-5-formyl tetrahydrofolate and L- over D-aminopterin.<sup>16,40</sup> Interestingly, folic acid is a poor substrate for RFC but is a good substrate for PCFT<sup>16,37</sup>; conversely,

the antifolates PT523 and GW1843U89 are excellent substrates for RFC but are poor substrates for PCFT.<sup>16,41</sup>

Other characteristics of PCFT were reported. Transport is not affected by the removal of Na<sup>+</sup>, K<sup>+</sup>, Ca<sup>2+</sup>, Mg<sup>2+</sup>, or Cl<sup>-</sup> but is decreased by treatment with a proton ionophore (carbonylcyano p-trifluoromethoxyphenylhydrazone)<sup>1</sup> or a K<sup>+</sup>/H<sup>+</sup> exchanging ionophore (nigericin).<sup>42</sup> Nitrate or bisulfite treatment of HeLa cells abolished the pH gradient and inhibited PCFT transport.<sup>43</sup> From studies in *Xenopus* oocytes, transport by PCFT is electrogenic with a net translocation of positive charges for each negatively charged folate molecule<sup>1</sup> accompanied by intracellular acidification.<sup>44</sup>

## 4 | PCFT STRUCTURE AND FUNCTION

PCFT belongs to the major facilitator superfamily (MFS) of transporters including the bacterial lactose/proton symporter (LacY), the inorganic phosphate/glycerol-3-phosphate antiporter (GlpT), and RFC.<sup>45,46</sup> hPCFT is composed of 459 amino acids (Figure 2) and shares ~14% of amino acid identity with hRFC.

Topology analyses of the hPCFT protein within the plasma membrane used substituted cysteine accessibility methods (SCAMs) with thiol-reactive reagents [e.g., 2-aminoethyl methanethiosulfonate (MTSEA)] to probe aqueous accessible residues/domains.<sup>47</sup> SCAM, combined with hemagglutinin (HA) labeling of the hPCFT N- and C-termini, defined 12 transmembrane domain (TMD) segments (illustrated in Figure 2).<sup>31,47,48</sup> Subsequent studies used SCAM with an expanded number of cysteine replacements to further refine the hPCFT topology including TMD boundaries and substrate-binding domains.<sup>49,50</sup> The hPCFT protein is glycosylated in the first extracellular loop at Asn58 and Asn68.<sup>48</sup> Loss of glycosylation upon treatment of cells with tunicamycin or mutation of Asn58 and Asn68 to Gln individually or together had only modest effects on hPCFT transport.<sup>48</sup>

Loss-of-function mutations in hPCFT from patients with HFM syndrome have been used to identify amino acids that may be structurally or functionally important.<sup>1,9,10,12,20,21,51-65</sup> Further interrogation of individual amino acids used systematic site-directed mutagenesis based on sequence conservation and predictions of membrane topology.<sup>44,54,65-77</sup> The computation of three-dimensional comparative protein structure models is feasible for MFS members with unknown structures based on previously solved MFS structures. For hPCFT, homology modeling based on the GlpT and GLUT5 structures has been useful for understanding PCFT structure and function, and for enabling predictions of the roles that

particular residues and domains play in hPCFT transport function.<sup>9-11</sup>

Amino acids in hPCFT implicated as functionally or structurally important by these approaches include Arg148, Asp109, Asp156, Glu185, Glu232, His281, Arg376, Tyr291, Tyr315, Tyr362, Tyr414, and Trp299.<sup>13,44,54,55,66-68</sup> Residues mapping to TMD2 (Gly93 and Phe94), TMD4 (Gly147, Ala152, Phe157, Gly158, and Leu161), TMD5 (Ile188), TMD7 (Ile278, His281, Phe282, Gly283, Ala284, Asp286, and Leu288), the TMD7-8 loop (Tyr291), TMD8 (Tyr315), TMD10 (Tyr362), and the lipid-aqueous interface (Trp48, Trp85, and Trp202) were identified by SCAM as potential substrate-binding domains.<sup>10,67-72</sup> Gly158 in TMD4 of hPCFT was identified as a target for sustained inhibition of transport by the flavonoid myricetin.<sup>78</sup>

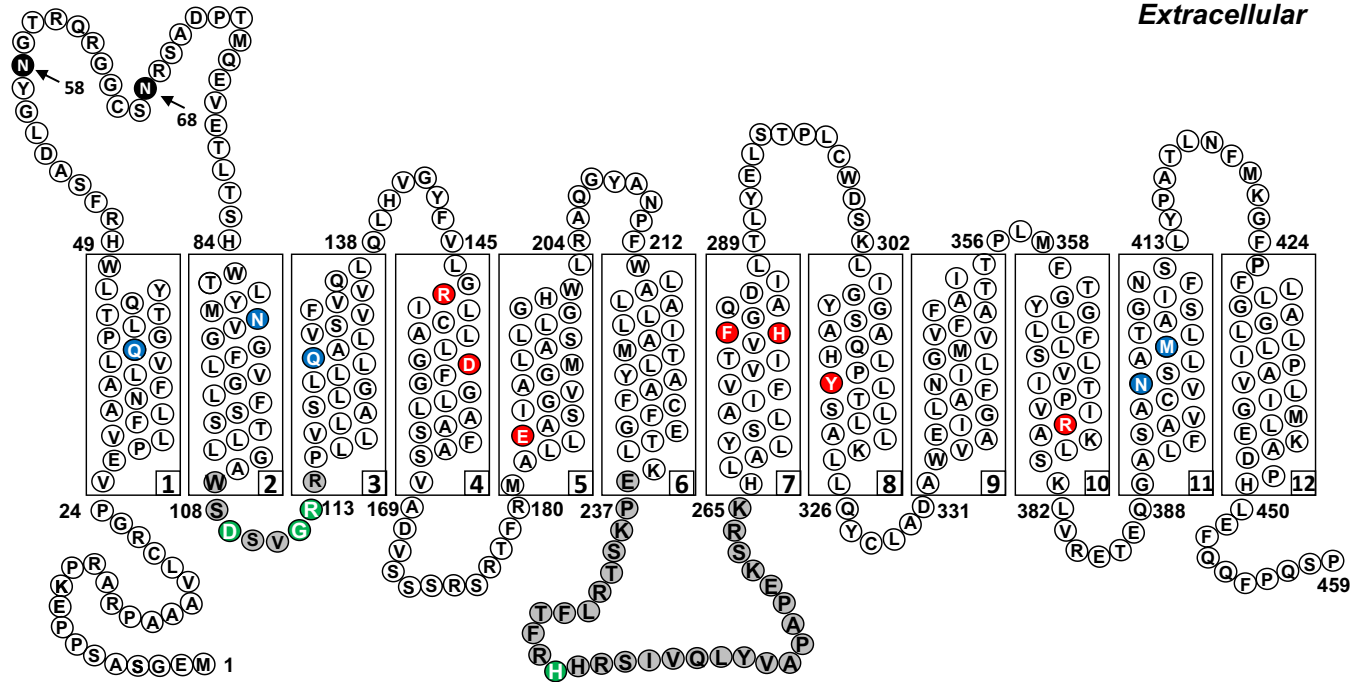
The conserved loop domain linking TMD2 and TMD3 (residues 109-114) is predicted to have a cytoplasmic orientation (Figure 2) and includes Asp109 and Arg113, neither of which can be replaced by other amino acids regardless of charge or polarity.<sup>12,54,70,73,74</sup> Likewise, Gly112 is required for transport function.<sup>70</sup> Mutations at Asp109 were reported to lock hPCFT in an “inward-open” conformation, as reflected in loss of accessibility of cysteine insertions to MTSEA-biotin by SCAM analysis and loss of transport function.<sup>75</sup> Interestingly, substitution of leucine at Gly305 (TMD8) in the mutant Asp109 hPCFT scaffold largely restored transport function and MTSEA-biotin accessibility.<sup>75</sup> Replacement of Phe392 (TMD11) with valine resulted in an analogous transport defective phenotype that was reversed by insertion of Leu at position 305.<sup>76</sup>

The hPCFT TMD2-3 loop domain includes a  $\beta$ -turn structure and was predicted by homology modeling based on the GlpT template to protrude into a hydrophobic cavity formed by TMDs 1, 3, 4, and 6.<sup>12</sup> Whereas the predicted cytosolic domain connecting TMDs 2 and 3 (positions 107-114) of hPCFT was reported to form a novel “reentrant loop” structure based on SCAM analysis with MTSEA-biotin,<sup>70</sup> in other reports Cys-substituted residues in this region showed limited accessibilities to extracellular sulfhydryl reagents.<sup>49,74</sup>

The hPCFT TMD6-7 loop domain is predicted to be intracellular (Figure 2) and includes a stretch of 30 mostly nonconserved residues (positions 236-265) with the exception of a conserved stretch of amino acids (RLFXXRH) from positions 241-247. The conserved His247 was implicated as functionally important, as amino acid substitutions (Ala, Arg, Gln, or Glu) at this position were associated with decreased transport compared to wild-type hPCFT.<sup>44</sup> By molecular modeling, His247 was predicted to reside at the cytoplasmic end of a solute pathway with hydrogen bonding to Ser172 where it restricts substrate access to the folate binding pocket.<sup>44</sup> Interestingly, in electrophysiological studies in *Xenopus* oocytes, the His247Ala mutant



Extracellular



Intracellular

**FIGURE 2** Schematic structure of hPCFT membrane topology. A topology model for hPCFT is shown based on the HMMTOP prediction algorithm and biochemical studies,<sup>47</sup> including 12 TMDs and internal N- and C-termini. N-Glycosylation sites at Asn58 and Asn68 are shown as black circles. Structurally and functionally important residues based on cPCFT structural studies<sup>13</sup> are labeled as blue and red circles. The residues labeled as red circles were validated with biochemistry studies on hPCFT, including Arg148,<sup>66,71</sup> Asp156,<sup>54,66</sup> Glu185,<sup>66</sup> His281,<sup>44</sup> Phe282,<sup>72</sup> Tyr315,<sup>10,67</sup> and Arg376.<sup>55,66</sup> The residues in the TMD 2-3 (positions 107–114) and TMD 6-7 (positions 236–265) loops are shown as gray circles, and specific residues (Asp109, Gly112, Arg113, and His247) in these domains implicated as functionally important by mutagenesis studies are highlighted in green<sup>12,44,70,74,75</sup>

dissociated folate and proton transport such that proton movement occurred without folate transport.<sup>44</sup>

The functional and mechanistic importance of the hPCFT TMD6-7 connecting loop was further studied by site-directed, deletion, and insertion mutagenesis.<sup>77</sup> Whereas removal of residues 252–265 from TMD7-12 abolished transport, chimeric proteins including non-homologous sequence replacements from a thiamine transporter (ThTr1) inserted into the hPCFT TMD6-7 loop region (positions 236 to 250, or 251 to 265; designated *tp*- and *pt*-hPCFT, respectively) were active; however, replacement of the entire TMD6-7 loop with ThTr1 sequence resulted in substantial loss of transport activity.<sup>77</sup> His247 replacements with Ala, Arg, Gln, and Glu, or His247 deletion, in wild-type hPCFT significantly suppressed transport,<sup>44</sup> yet the same His247 replacements in *pt*-hPCFT showed no obvious effect on transport activity.<sup>77</sup> Thus, the impact of His247 substitutions on hPCFT transport appears to be context dependent and varies with the flanking sequence and secondary structure. Indeed, the role of the TMD6-7 loop domain in hPCFT function appears to be largely unrelated to specific primary sequence elements, as long as sufficient secondary structure

is preserved and proper spacing between the TMD1-6 and TMD7-12 segments is ensured to maintain protein stability and to facilitate optimal membrane translocation. Consistent with this notion, hPCFT could be coexpressed as TMD1–6 and TMD7-12 half-molecules to restore transport activity, albeit in low levels.<sup>77</sup>

## 5 | STRUCTURAL BIOLOGY OF PCFT

Characterization of PCFT structure is essential to understanding critical determinants of substrate binding and the mechanism of membrane transport. Only a few crystallographic structures of eukaryotic MFS proteins have been reported, for example, PiPT,<sup>79</sup> GLUT1,<sup>80</sup> GLUT3,<sup>81</sup> SERT,<sup>82</sup> and ENT1.<sup>83</sup> However, there are numerous examples of prokaryotic MFS transporters for which structures have been resolved, for example, LacY,<sup>84</sup> GltT,<sup>85</sup> EmrD,<sup>86</sup> and YajR.<sup>87</sup> MFS transporters share a conserved core fold that comprises 12 transmembrane segments organized into two discretely folded N- and C-terminal domains. Within each domain, six consecutive

transmembrane segments are folded into a pair of “3+3” inverted repeats.<sup>88–90</sup>

Recently, cryo-electron microscopy (cryo-EM) structures of the chicken PCFT (cPCFT) in a substrate-free state (3.2 Å) and in complex with the antifolate pemetrexed (3.3 Å) were reported.<sup>13</sup> These findings provide a structural basis for understanding (anti)folate recognition and enable insights into the pH-regulated mechanism of folate transport mediated by PCFT. The cryo-EM structure shows that the cPCFT protein adopts the canonical MFS fold in an “outward-open” conformation.<sup>13</sup> TMDs 1, 2, 4, 5, 7, 8, 10, and 11 form a hydrophilic cavity for binding anionic folate substrates, with TMDs 1, 2, 7, and 8 forming an open extracellular gate, and TMDs 4, 5, 10, and 11 forming a closed intracellular gate. Two salt bridges form in the cPCFT protein, between Arg156 and Asp164, and between Glu193 and Arg384 (Figure 3A,B lists the homologous amino acid residues between cPCFT and hPCFT). These salt bridge interactions serve to stabilize the transporter in the outward-open state. In addition, a hydrogen-bond interaction between His289 in TMD7 and Asn350 in TM9 in cPCFT stabilizes the extracellular gate in the outward-open state. The extracellular and intracellular gates are suggested to alternate between open (splayed apart) and closed (packed together) states during transport,<sup>13</sup> as for other members of the MFS.<sup>85,90</sup>

To understand the structural determinants of recognition and transport of (anti)folate substrates, a structure of cPCFT in complex with pemetrexed was determined at a resolution of 3.3 Å.<sup>13</sup> Pemetrexed (Figure 4) is one of the best substrates for hPCFT<sup>16,28</sup> and has similar affinities for binding to hPCFT and cPCFT.<sup>13</sup> To mimic the acidic conditions for optimal transport, the structure of the cPCFT/pemetrexed complex was determined at pH 6.0. Pemetrexed was well-resolved in the cryo-EM maps of cPCFT and bound in a kinked conformation at the base of a polar cavity composed of both N- and C-terminal bundles. The pyrimidine moiety of pemetrexed sits in a polar cavity constructed from side chains in the C-terminal bundle (Figure 3C). The carbonyl and 3-nitrogen of the pyrimidine ring of pemetrexed interact with Tyr323 in TMD8 of cPCFT, and the 2-amino group of the pyrimidine interacts with Glu193 in TMD5. The pyrrole nitrogen of pemetrexed interacts with Glu407 in TMD11 and the side-chain benzoyl group makes a  $\pi$ - $\pi$  stacking interaction with Phe290 in TMD7 of cPCFT. The L-glutamate  $\gamma$ -carboxylate group of pemetrexed interacts with Arg156 in TMD4 and Asn98 in TMD2 in a positively charged pocket located within the N-terminal bundle of cPCFT. Whereas the  $\alpha$ -carboxylate of the L-glutamate of pemetrexed does not show specific interactions with side chains in the binding site, both the amide and carbonyl groups adjacent to the benzoyl ring interact with Ser411 in TMD11 of cPCFT (Figure 3C).

The cPCFT structure also sheds new light on important determinants for binding and transport of PCFT-targeted drugs for cancer with selectivity over RFC<sup>2,8</sup> based on published studies of 6-substituted pyrrolo[2,3-*d*]pyrimidine thienoyl antifolates with different bridge lengths ranging from one to six carbons,<sup>91,92</sup> for which the compounds with 3- (AGF94) or 4- (AGF71) bridge carbons (Figure 4) appear to be optimal. The structural model for cPCFT predicts that bound pemetrexed coordinates with Arg156 at the  $\gamma$ -carboxylate and Glu193 at the 2-amino group on the pyrimidine ring, thus defining a minimal distance between these two key residues in the PCFT binding site for related (anti)folate substrates (Figure 3D). Lengthening the bridge from two carbons as in pemetrexed (a 5-substituted pyrrolo[2,3-*d*]pyrimidine antifolate) to three or four carbons as in AGF94 and AGF71 would result in the  $\gamma$ -carboxylate of the bound ligand extending into a conserved polar pocket which contains Gln43 in TMD1 and Gln135 in TMD3 of cPCFT (Figure 3D).<sup>13</sup> The net effect would be that the  $\alpha$ -carboxylate of the bound substrate would be forced to interact with Arg156 *in lieu* of the  $\gamma$ -carboxylate.<sup>13</sup> Decreasing the bridge length to less than three carbons or greater than five carbons would result in inactive compounds of this series,<sup>91,92</sup> most likely due to loss of PCFT binding and transport. Clearly, the structure-based pharmacophore provides an important framework for rational drug design to provide high levels of PCFT transport.

## 6 | ALTERNATING-ACCESS TRANSPORT MECHANISM OF PCFT

MFS transporters are generally believed to facilitate transport via an “alternating access” mechanism,<sup>88,90</sup> whereby the substrate-binding site is alternately accessible from either side of the membrane via conformational changes in the transporter. This is generally viewed as involving four distinct stages.<sup>88</sup> The transport cycle starts with an outward facing “unloaded” state (*step 1*). The binding of substrate triggers a conformational change that results in a membrane transition from an outward to an inward facing state (*step 2*). This is followed by release of substrate into the cytoplasm (*step 3*) and finally a return to the unloaded outward facing state to complete the transport cycle (*step 4*). The recent apo- and ligand-bound structures of cPCFT,<sup>13</sup> combined with extensive published hPCFT mutant studies,<sup>44,54,65–77</sup> provide an increasingly detailed model for proton-coupled folate transport via PCFT.

The cryo-EM structure of cPCFT<sup>13</sup> shows that cPCFT adopts a canonical MFS fold in an outward-open conformation stabilized by an intrahelical salt bridge between

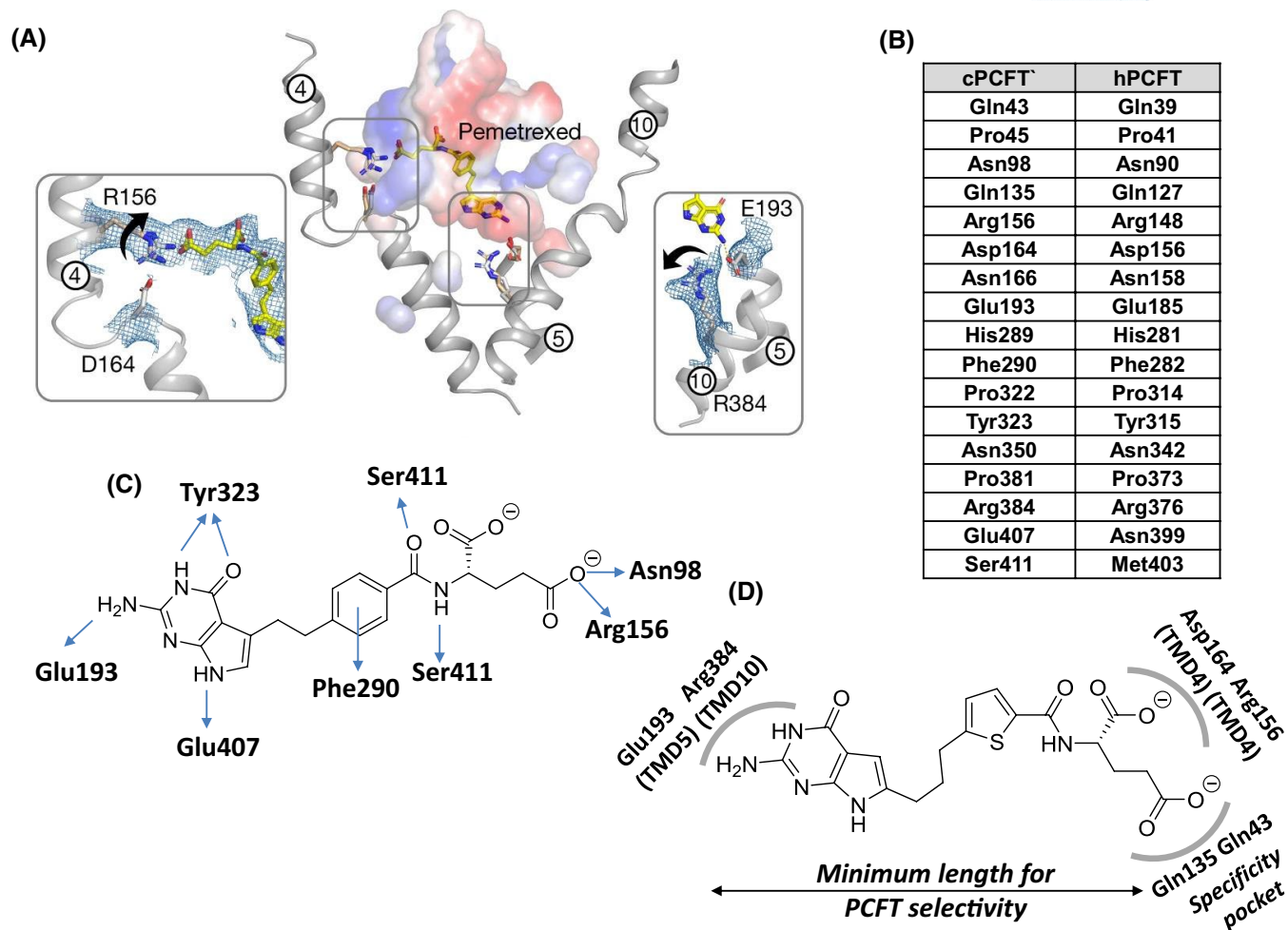


**FIGURE 3** cPCFT structure and identification substrate-binding site. (A) Key side-chain rearrangements are observed after pemetrexed and proton binding with cPCFT. The insets show the cryo-EM density of cPCFT for the two salt-bridge interactions, which are broken in the presence of substrate. Arrows indicate the direction of side-chain movement. TMDs 4, 5, and 10 in cPCFT are indicated. This panel is from the publication by Parker et al.<sup>13</sup> with copyright permission. (B) A table is provided listing key residues in the cPCFT structure and their counterparts in hPCFT. (C) Schematic of the deduced binding pose of cPCFT for pemetrexed based on the cPCFT/pemetrexed structure.<sup>13</sup> This panel is adapted from that in the publication by Parker et al.<sup>13</sup> (D) Predicted binding interactions of AGF94 with cPCFT. AGF94 is a 6-substituted pyrrolo[2,3-*d*]pyrimidine preclinical compound with three-carbon chain bridge length<sup>92</sup> (Figure 4). AGF94 can engage both salt bridges of cPCFT at either end of the binding site, resulting in an opening of the intracellular gate, along with the specificity pocket for PCFT substrate binding. This panel is adapted from that in the publication by Parker et al.<sup>13</sup>

Arg156 and Asp164 in TMD4, an interhelical salt bridge between Glu193 in TMD5 and Arg384 in TMD10, and a hydrogen bond between His289 in TMD7 and Asn350 in TMD9. In this conformation, a hydrophilic cavity for binding of anionic (anti)folate substrates is generated (Figure 3C). Consistent with the anionic character of (anti)folates ( $-2$  charge at physiological pH),<sup>93</sup> the entrance to the transporter binding site is positively charged. This feature may serve to attract folates and related molecules and funnel them into the transporter.<sup>13</sup>

The presence of intrahelical and interhelical salt bridges in PCFT suggests a mechanism within the MFS fold for coupling (anti)folate transport to pH gradients across the membrane. Based on the cryo-EM structure

of cPCFT,<sup>13</sup> a detailed mechanism for transport of pemetrexed at acidic pH can be envisaged (Figure 5). In the outward open state (*step 1*), protonation of Asp164 and Glu193 in cPCFT weakens the salt bridge network formed between side chains of Arg156 and Asp164, and between Glu193 and Arg384. Pemetrexed binding to cPCFT further weakens the salt bridges by inducing increased pKa values for Asp164 and Glu193<sup>13</sup> (*step 2*). As a result, a salt bridge forms between the pemetrexed  $\gamma$ -carboxylate group and Arg156, and the 2-amine group on the pyrimidine ring of pemetrexed associates with Glu193 in cPCFT (Figure 3C). An additional effect of pemetrexed binding involves disruption of the hydrogen bond between His289 in TMD7 and Asn350 in TMD9 of

cPCFT. Protonation of His289 facilitates the interaction between the benzoyl group of pemetrexed and Phe290 and repositioning of TMD7 toward TMD1 to initiate closure of the extracellular gate<sup>13</sup> (*step 3*). Hence, ligand binding dictates the conformational changes in the cPCFT protein required for transport. At the cytoplasmic gate, binding of pemetrexed with cPCFT triggers the cytoplasmic half of TMD4 and TMD5 to open, releasing the antifolate into the cell (*step 4*). This is accompanied by deprotonation of Asp164, Glu193, and His289 and reformation of the salt bridge and hydrogen bond networks, resulting in reorientation of the carrier to the outward-facing state (*step 5*).

This mechanism accounts for the pH dependence of PCFT transport including how protons facilitate (anti) folate transport into cells. Topological analyses predict breaks in four of the hPCFT transmembrane helices.<sup>21</sup> Three of the breaks contain a Pro residue in hPCFT (Pro41, Pro314, and Pro373 in TMDs 1, 8, and 10, respectively); the break in TMD4 involves Gly158. These breaks likely enable the oscillation of the carrier between the inward-open and outward-open conformational states requisite for transport.<sup>94</sup>

While the cryo-EM structure of cPCFT validates mechanistically important roles of Arg148, Glu185, His281, Phe282, Tyr315, and Arg376 in hPCFT transport (Figure 3B) suggested from biochemical studies of hPCFT,<sup>10,44,54,66,67,71,72</sup> there remain some uncertainties. For example, the cryo-EM structure of cPCFT demonstrates an intrahelical salt bridge between Arg156 and Asp164 within TMD4 of cPCFT and protonation of Asp164 upon substrate binding<sup>13</sup>; however, a functional role for Asp156 in hPCFT transport (corresponds to Asp164 in cPCFT; Figure 3B) has not been demonstrated.<sup>65</sup> Rather, Asp156 appeared to be important for hPCFT protein stability.<sup>65</sup> Furthermore, no mechanistic roles of the TMD2-3 intracellular loop,<sup>12,54,70,73,74</sup> and possibly His247,<sup>44,77</sup> in hPCFT transport function were suggested from the cryo-EM structure.<sup>13</sup> These questions may not be resolved until a structure of hPCFT becomes available.

## 7 | OLIGOMERIC STRUCTURE OF HPCFT AND ITS FUNCTIONAL IMPORTANCE

An additional consideration in the structure and function of PCFT involves the potential role of PCFT oligomerization (Figure 1). Numerous MFS proteins have been reported to form oligomers (e.g., dimers, tetramers), including LacS, AE1, GLUT1, TetA, and hRFC.<sup>95–101</sup> For hPCFT, formation of homo-oligomers could be significant to the mechanism of transport and its regulation.

Based on comprehensive studies using a wide range of methods including protein cross-linking, blue native gel electrophoresis, nickel affinity chromatography, and fluorescence resonance energy transfer (FRET), hPCFT was concluded to form homo-oligomers, with the hPCFT dimer as the dominant form both in detergent solution and *in situ*.<sup>102</sup> hPCFT oligomers were also identified by Zhao et al. by homo-bifunctional cross-linking<sup>69</sup> and by Aduri et al. from size exclusion chromatography following solubilization with lauryl maltose neopentyl glycol (LMNG).<sup>103</sup> LMNG-solubilized hPCFT bound folate and appeared to be a dimer by size exclusion which was further supported by negative electron microscopy on the LMNG preparation that showed that hPCFT was the predicted size of a dimer.<sup>103</sup>

However, in other studies, the predominant form of hPCFT expressed in Sf9 insect cells and oocytes and solubilized in n-dodecyl- $\beta$ -D-maltoside (DDM) appeared to be a monomer,<sup>104</sup> a result subsequently confirmed by Aduri et al.<sup>103</sup> Duddempudi et al.<sup>104</sup> also reported evidence purported to suggest the existence of monomeric hPCFT, including blue native electrophoresis and chemical cross-linking with glutaraldehyde and dimethyl adipimidate. However, given the methodologic differences in membrane preparations and detergent solubilization, let alone use of different cross-linking agents, it is difficult to reconcile the findings of Duddempudi et al.<sup>104</sup> with those suggesting that hPCFT occurs as an oligomer, most likely a dimer.<sup>69,101,103,105</sup>

A possible explanation for these different findings may involve a weak association between hPCFT monomers and the essential role of the membrane lipids in promoting oligomer formation. Gupta et al. used mass spectrometry to simultaneously determine the presence of interfacial lipids and oligomeric stability of membrane proteins and to assess how lipids may impact membrane protein–protein associations.<sup>106</sup> Lipid binding was obligatory for dimerization of membrane proteins (e.g., NhaA). Correlations between the interfacial strength of association and the presence of interfacial lipids accounted for interactions within a number of  $\alpha$ -helical membrane proteins. Indeed, this could explain why many MFS transporters such as GLUT transporters were reported to exist as oligomers in membranes,<sup>98,107</sup> yet nonetheless have been extracted, purified, and crystallized in detergent as monomers.<sup>80,81,108</sup>

One of the most compelling arguments for a functional role of hPCFT dimerization involves studies by Hou et al.<sup>102</sup> In this report, co-expression of wild-type and inactive mutant Pro425Arg hPCFTs in hPCFT-null HeLa cells resulted in a distinctive “dominant-positive” transport phenotype, best interpreted as positive cooperativity between wild-type and mutant hPCFT monomers



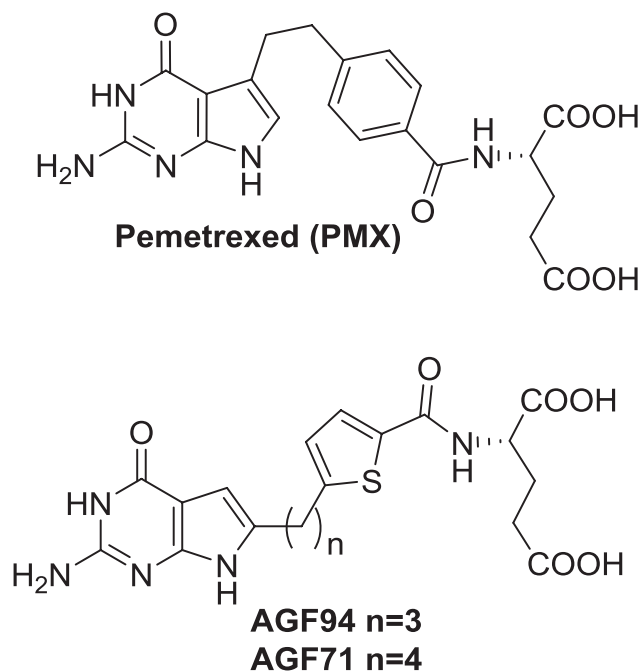


**FIGURE 4** Structures for pemetrexed and AGF94 and AGF71. Pemetrexed is a clinically used 5-substituted pyrrolo[2,3-d]pyrimidine antifolate.<sup>128</sup> AGF71<sup>91</sup> and AGF94<sup>92</sup> are preclinical 6-substituted pyrrolo[2,3-d]pyrimidine antifolates with demonstrated specificity for transport by PCFT over RFC

and functional “rescue” of mutant hPCFT by wild-type hPCFT.<sup>102</sup> Similar “cooperative” phenotypes were reported for other MFS members, including the dimeric lactose transporter LacS for which coexpression of non-functional mutant LacS with wild-type protein abolished H<sup>+</sup>-active transport.<sup>95</sup>

Additional studies investigated structural determinants of hPCFT oligomerization. Although the transmembrane sequence motif GXXXG has been implicated to facilitate tight interactions between transmembrane  $\alpha$ -helices,<sup>109–112</sup> including dimerization of membrane proteins,<sup>113–119</sup> the two GXXXG motifs in hPCFT (located in TMDs 2 and 4) are not directly involved in hPCFT oligomerization, as suggested by nickel affinity chromatography and FRET experiments.<sup>105</sup> Rather, these GXXXG motifs seem likely to play a role in stability and intracellular trafficking of hPCFT.<sup>105</sup>

Zhao et al. used homo-bifunctional cross-linking [1,1-methanediyl bismethanethiosulfonate (MTS-1-MTS)] between Cys229 (located in TMD6) in individual hPCFT monomers, implicating an interface involving TMD6 between hPCFT monomers. In additional studies, hPCFT cysteine insertion mutants in TMD3 (Q136C and L137C) and TMD6 (W213C, L214C, L224C, A227C, F228C, F230C, and G231C) were expressed in hPCFT-null HeLa cells and cross-linked with 1,6-hexanediyl bismethanethiosulfonate, confirming TMD juxtapositions. This

implies that TMDs 3 and 6 provide critical interfaces for formation of hPCFT oligomers, which might be facilitated by the GXXXG motifs in TMD2 and TMD4.<sup>105</sup>

Based on the “alternate access model” for secondary transporters such as LacY,<sup>84</sup> an analogous reaction scheme for hPCFT-mediated transport was proposed which incorporates a functional impact of hPCFT oligomerization<sup>102</sup> (Figure 6). In this model, both hPCFT monomers in homodimeric hPCFT are assumed to undergo the transport cycle concurrently via six distinct stages. The scheme starts with an outward facing unloaded hPCFT dimer composed of two wild-type monomers. The ordered binding of co-transported protons (*step 1*) and substrates (*step 2*) to both monomers triggers a conformational change that results in a membrane transition of hPCFT monomers from an outward to an inward facing state (*step 3*). This is followed by an ordered release of substrates (*step 4*) and protons (*step 5*) from both hPCFT monomers into the cytoplasm and, finally, return of both unloaded hPCFT monomers to their outward facing state to complete the transport cycle (*step 6*). Intrinsic to this model is functional cooperativity between associated hPCFT monomers suggested by the studies of Hou et al.<sup>102</sup>

## 8 | FUTURE DIRECTIONS

This review summarizes major advances in the biology of PCFT. PCFT was discovered in 2006 and identified as the major folate transporter involved in the intestinal absorption of dietary folate such that loss of PCFT was causal in a rare autosomal condition called HFM.<sup>1</sup> Subsequent studies confirmed the high-level hPCFT expression in tumors,<sup>3,5–7,25</sup> prompting interest in developing PCFT-targeted cytotoxic drugs<sup>2,8,28</sup> that draw from its substantial activity at the acidic pH associated with the microenvironment of tumors. Studies began to explore the transcriptional regulation of hPCFT including identification of key transcription factors and the role of promoter hypermethylation as important determinants of differential hPCFT expression between tissues and tumors.<sup>4,29,30,32,33,35,36,120</sup> Evidence that hPCFT can form homo-oligomers,<sup>69,102,103</sup> suggested yet another potential level of regulation, including the possibility that heterozygous hPCFT variants in HFM patients could impact trafficking and transport function of wild-type carrier via the formation of variant/wild-type oligomers<sup>102</sup> (Figure 1 shows various modes of PCFT regulation as described in this review).

Over the past 15 years, the progress in understanding the biology of PCFT and its clinical importance and therapeutic potential has been staggering. Particularly notable is the extent to which characterization of the causal basis for HFM<sup>1,9,12,20,21,51–64</sup> has shed light on PCFT structure

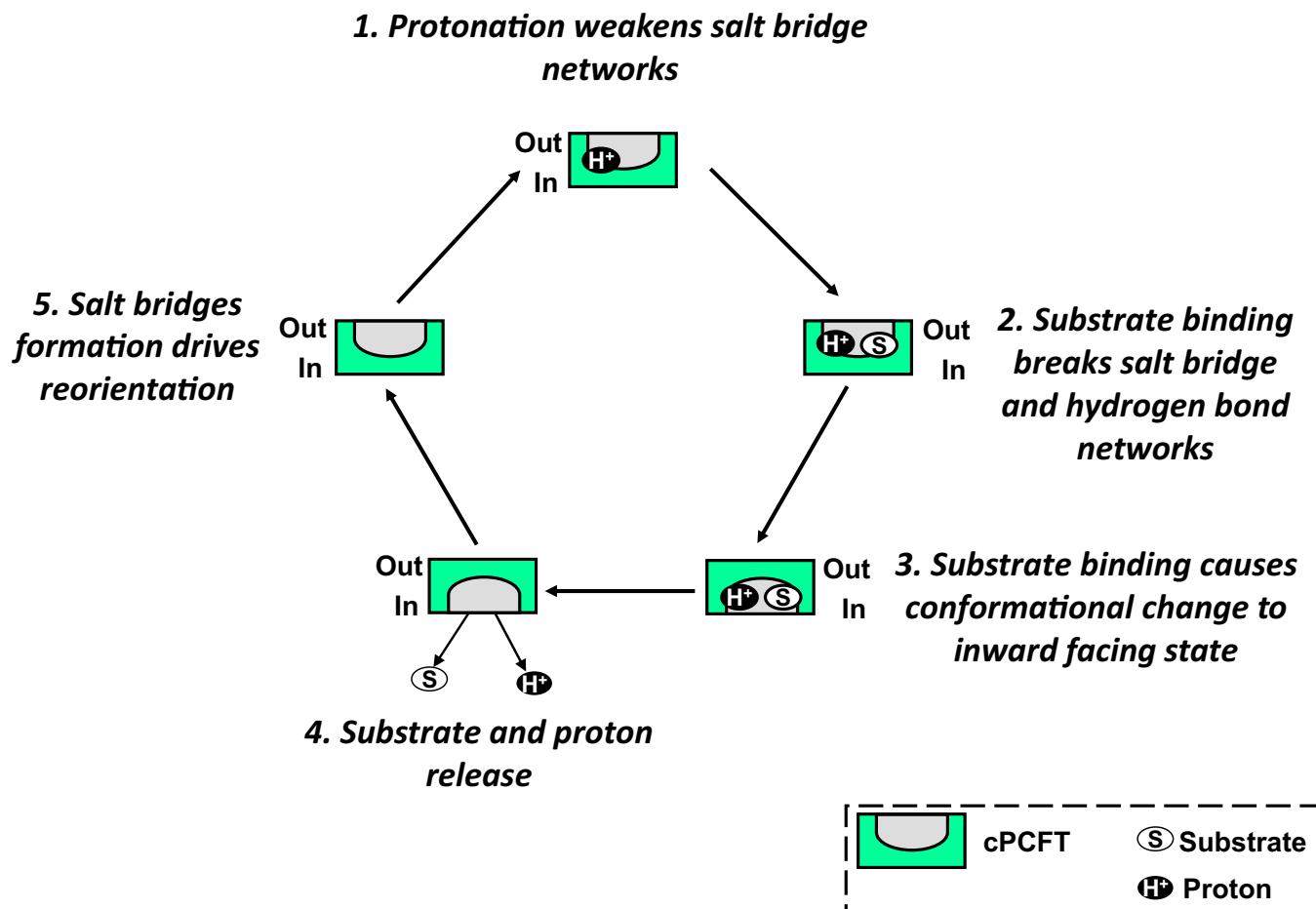


**FIGURE 5** Key steps in the alternating-access model for cPCFT. Based on the “alternate access model” for secondary transporters<sup>88,90</sup> and the cryo-EM structure of cPCFT,<sup>13</sup> a model of cPCFT transport is depicted. In the outward open state of cPCFT at acidic pH, the protein is primed for transport upon protonation of Asp164 and Glu193 (*step 1*). Proton binding drives transport and facilitates movement of the gating helices. Binding of the ligand promotes closure of the extracellular gate (*step 2*) through an interaction of the ligand with Phe290 on TMD7 and is facilitated by the protonation of His289. Substrate binding causes a conformational change to an inward facing state (*step 3*). The interaction with ligand triggers the intracellular gate to open, releasing protons and the (anti)folate substrate into the cell (*step 4*). Deprotonation of Asp164, Glu193 and His289 favors the reformation of the salt bridges and hydrogen-bond networks and drives reorientation to the outward-facing state (*step 5*). This mechanism explains the pH dependency of PCFT<sup>57</sup> and how protons facilitate (anti) folate transport into the cell

and mechanism, including the identification of mechanistically important residues and regions involved in substrate binding or proton coupling. Of course, the availability of cryo-EM structures of cPCFT in its apo form and in complex with the pemetrexed<sup>13</sup> provides exciting new opportunities to interpret the extensive mutant studies on hPCFT<sup>44,54,65–77</sup> in light of critical determinants of (anti) folate binding and the mechanism of (anti)folate transport mediated by PCFT. The structure-based pharmacophore for PCFT<sup>13</sup> establishes an important new framework for further rational design of PCFT-selective antifolates for tumor targeting and decreased toxicity to normal tissues which express substantial RFC without PCFT. This will complement ongoing studies with multiparameter optimization and medicinal chemistry to discover the next generation of PCFT-targeted agents. Looking forward,

these concepts will be advanced immeasurably by solving an RFC structure.

While hPCFT-selective antifolates have been identified<sup>2,8,28</sup> (without transport by RFC), their efficacy could be further optimized by modulating hPCFT expression at the transcriptional level with demethylating agents<sup>25</sup> or other approaches. It will be additionally important to further confirm the larger role of hPCFT oligomerization, including its overall functional and regulatory importance. This extends to critical structural determinants including the impact of interfacial lipids on hPCFT dimerization, as these could enable development of strategies to modulate oligomerization, along with the use of pharmacologic chaperones such as small molecules or peptidomimetics that promote trafficking and increase transporter expression and function.

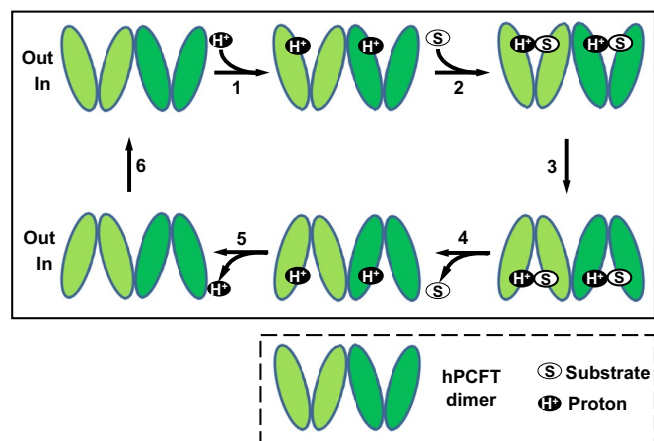


**FIGURE 6** Proposed reaction scheme for hPCFT-mediated cellular uptake involving cooperative interactions between hPCFT monomers. Based on the “alternate access model” for secondary transporters, such as LacY,<sup>84</sup> adapted from that of Unal et al.<sup>66</sup> for monomeric hPCFT, an analogous reaction scheme is depicted for hPCFT-mediated transport that incorporates the functional impact of hPCFT oligomerization (dimerization). The model starts from the outward facing unloaded dimer (each hPCFT monomer is depicted as TMD1–6 and TMD7–12 segments), followed by the ordered binding of the co-transported protons (*step 1*) and (anti) folate substrates (*step 2*), which triggers a conformational change resulting in simultaneous transition of the two hPCFT monomers to an inward facing state (*step 3*). This is followed by an ordered release of substrates (*step 4*) and protons (*step 5*) into the cytoplasm. The unloaded homo-oligomeric unit then returns to the outward facing state (*step 6*) to complete the transport cycle. In this model, the two hPCFT monomers are suggested to function cooperatively in facilitating substrate and proton binding, conformational changes, and substrate and proton release. This figure was adapted from that in Hou et al.<sup>102</sup>

Heterologous protein interactions could also play an important role in hPCFT regulation as protein interaction networks (“interactome”) are important for processes critical to cellular homeostasis<sup>121,122</sup> (depicted in Figure 1). Macromolecular assemblies involving membrane proteins are of particular interest as these serve vital biological roles and provide potential drug targets.<sup>123</sup> Proteins interacting with hPCFT could be identified by “proximity-dependent biotin identification” (BioID) methods, and their interaction with hPCFT could then be verified by co-immunoprecipitation and functional studies (e.g., gene knock-outs).<sup>124,125</sup>

For hPCFT, protein–protein homo and hetero interactions might explain anomalies such as the basis for an intracellular PCFT fraction reported in multiple studies,<sup>57,126</sup> the negative impact of increasing hRFC on hPCFT activity,<sup>38</sup> and the “disconnect” between levels of endogenous hPCFT proteins and hPCFT transport activity described in human tumor cell lines.<sup>127</sup>

## DISCLOSURES

The authors have stated explicitly that there is no conflict of interest in connection with this article.

## AUTHOR CONTRIBUTIONS

Zhanjun Hou and Larry H. Matherly wrote the paper. Aleem Gangjee consulted on the chemistry and assisted with the writing of the manuscript.

## ORCID

Zhanjun Hou  <https://orcid.org/0000-0001-5631-5202>

## REFERENCES

1. Qiu A, Jansen M, Sakaris A, et al. Identification of an intestinal folate transporter and the molecular basis for hereditary folate malabsorption. *Cell*. 2006;127:917-928.
2. Matherly LH, Hou Z, Gangjee A. The promise and challenges of exploiting the proton-coupled folate transporter for selective therapeutic targeting of cancer. *Cancer Chemother Pharmacol*. 2018;81:1-15.
3. Hou Z, Gattoc L, O'Connor C, et al. Dual targeting of epithelial ovarian cancer via folate receptor alpha and the proton-coupled folate transporter with 6-substituted pyrrolo[2,3-d]pyrimidine antifolates. *Mol Cancer Ther*. 2017;16:819-830.
4. Giovannetti E, Zucali PA, Assaraf YG, et al. Role of proton-coupled folate transporter in pemetrexed resistance of mesothelioma: clinical evidence and new pharmacological tools. *Ann Oncol*. 2017;28:2725-2732.
5. Wilson MR, Hou Z, Yang S, et al. Targeting nonsquamous non-small cell lung cancer via the proton-coupled folate transporter with 6-substituted pyrrolo[2,3-d]pyrimidine thienoyl antifolates. *Mol Pharmacol*. 2016;89:425-434.
6. Kugel Desmoulin S, Wang L, Hales E, et al. Therapeutic targeting of a novel 6-substituted pyrrolo [2,3-d]pyrimidine thienoyl antifolate to human solid tumors based on selective uptake by the proton-coupled folate transporter. *Mol Pharmacol*. 2011;80:1096-1107.
7. Dekhne AS, Ning C, Nayeem MJ, et al. Cellular pharmacodynamics of a novel pyrrolo[3,2-d]pyrimidine inhibitor targeting mitochondrial and cytosolic one-carbon metabolism. *Mol Pharmacol*. 2020;97:9-22.
8. Kugel Desmoulin S, Hou Z, Gangjee A, Matherly LH. The human proton-coupled folate transporter: biology and therapeutic applications to cancer. *Cancer Biol Ther*. 2012;13:1355-1373.
9. Aluri S, Zhao R, Lubout C, Goorden SMI, Fiser A, Goldman ID. Hereditary folate malabsorption due to a mutation in the external gate of the proton-coupled folate transporter SLC46A1. *Blood Advances*. 2018;2:61-68.
10. Aluri S, Zhao R, Fiser A, Goldman ID. Residues in the eighth transmembrane domain of the proton-coupled folate transporter (SLC46A1) play an important role in defining the aqueous translocation pathway and in folate substrate binding. *Biochem Biophys Acta*. 2017;1859:2193-2202.
11. Zhao R, Najmi M, Fiser A, Goldman ID. Identification of an extracellular gate for the proton-coupled folate transporter (PCFT-SLC46A1) by cysteine cross-linking. *J Biol Chem*. 2016;291:8162-8172.

12. Lasry I, Berman B, Straussberg R, et al. A novel loss-of-function mutation in the proton-coupled folate transporter from a patient with hereditary folate malabsorption reveals that Arg 113 is crucial for function. *Blood*. 2008;112:2055-2061.
13. Parker JL, Deme JC, Kuteyi G, et al. Structural basis of antifolate recognition and transport by PCFT. *Nature*. 2021;595:130-134.
14. Wang Y, Zhao R, Goldman ID. Characterization of a folate transporter in HeLa cells with a low pH optimum and high affinity for pemetrexed distinct from the reduced folate carrier. *Clin Cancer Res*. 2004;10:6256-6264.
15. Alam C, Kondo M, O'Connor DL, Bendayan R. Clinical implications of folate transport in the central nervous system. *Trends Pharmacol Sci*. 2020;41:349-361.
16. Zhao R, Goldman ID. The molecular identity and characterization of a Proton-coupled Folate Transporter—PCFT; biological ramifications and impact on the activity of pemetrexed. *Cancer Metastasis Rev*. 2007;26:129-139.
17. Said HM, Smith R, Redha R. Studies on the intestinal surface acid microclimate: developmental aspects. *Pediatr Res*. 1987;22:497-499.
18. McEwan GT, Lucas ML, Denvir M, et al. A combined TDDA-PVC pH and reference electrode for use in the upper small intestine. *J Med Eng Technol*. 1990;14:16-20.
19. Counillon L, Pouysségur J. The expanding family of eucaryotic Na<sup>+</sup>/H<sup>+</sup>exchangers. *J Biol Chem*. 2000;275:1-4.
20. Tozawa Y, Abdrabou S, Nogawa-Chida N, et al. A deep intronic mutation of c.1166-285 T > G in SLC46A1 is shared by four unrelated Japanese patients with hereditary folate malabsorption (HFM). *Clin Immunol (Orlando, FL)*. 2019;208:108256.
21. Zhao R, Aluri S, Goldman ID. The proton-coupled folate transporter (PCFT-SLC46A1) and the syndrome of systemic and cerebral folate deficiency of infancy: hereditary folate malabsorption. *Mol Aspects Med*. 2017;53:57-72.
22. Umapathy NS, Gnana-Prakasam JP, Martin PM, et al. Cloning and functional characterization of the proton-coupled electrogenic folate transporter and analysis of its expression in retinal cell types. *Invest Ophthalmol Vis Sci*. 2007;48:5299-5305.
23. Caviedes L, Iniguez G, Hidalgo P, et al. Relationship between folate transporters expression in human placentas at term and birth weights. *Placenta*. 2016;38:24-28.
24. Zhao R, Matherly LH, Goldman ID. Membrane transporters and folate homeostasis: intestinal absorption and transport into systemic compartments and tissues. *Expert Rev Mol Med*. 2009;11:e4.
25. Giovannetti E, Zucali PA, Assaraf YG, et al. Role of proton-coupled folate transporter in pemetrexed resistance of mesothelioma: clinical evidence and new pharmacological tools. *Ann Oncol*. 2017;28(11):2725-2732.
26. Cohen MH, Cortazar P, Justice R, Pazdur R. Approval summary: pemetrexed maintenance therapy of advanced/metastatic nonsquamous, non-small cell lung cancer (NSCLC). *Oncologist*. 2010;15:1352-1358.
27. Cohen MH, Justice R, Pazdur R. Approval summary: pemetrexed in the initial treatment of advanced/metastatic non-small cell lung cancer. *Oncologist*. 2009;14:930-935.
28. Matherly LH, Wilson MR, Hou Z. The major facilitative folate transporters SLC19A1 and SLC46A1: biology and role in antifolate chemotherapy of cancer. *Drug Metab Dispos Biol Fate Chem*. 2014;42:632-649.
29. Diop-Bove NK, Wu J, Zhao R, Locker J, Goldman ID. Hypermethylation of the human proton-coupled folate transporter (SLC46A1) minimal transcriptional regulatory region in an antifolate-resistant HeLa cell line. *Mol Cancer Ther*. 2009;8:2424-2431.
30. Gonen N, Bram EE, Assaraf YG. PCFT/SLC46A1 promoter methylation and restoration of gene expression in human leukemia cells. *Biochem Biophys Res Commun*. 2008;376:787-792.
31. Qiu A, Min SH, Jansen M, et al. Rodent intestinal folate transporters (SLC46A1): secondary structure, functional properties, and response to dietary folate restriction. *Am J Physiol Cell Physiol*. 2007;293:C1669-C1678.
32. Gonen N, Assaraf YG. The obligatory intestinal folate transporter PCFT (SLC46A1) is regulated by nuclear respiratory factor 1. *J Biol Chem*. 2010;285:33602-33613.
33. Stark M, Gonen N, Assaraf YG. Functional elements in the minimal promoter of the human proton-coupled folate transporter. *Biochem Biophys Res Commun*. 2009;388:79-85.
34. Yamamoto J, Ikeda Y, Iguchi H, et al. A Kruppel-like factor KLF15 contributes fasting-induced transcriptional activation of mitochondrial acetyl-CoA synthetase gene AceCS2. *J Biol Chem*. 2004;279:16954-16962.
35. Eloranta JJ, Zair ZM, Hiller C, Hausler S, Stieger B, Kullak-Ublick GA. Vitamin D3 and its nuclear receptor increase the expression and activity of the human proton-coupled folate transporter. *Mol Pharmacol*. 2009;76:1062-1071.
36. Hou Z, O'Connor C, Fruhauf J, et al. Regulation of differential proton-coupled folate transporter gene expression in human tumors: transactivation by KLF15 with NRF-1 and the role of Sp1. *Biochem J*. 2019;476:1247-1266.
37. Matherly LH, Hou Z, Deng Y. Human reduced folate carrier: translation of basic biology to cancer etiology and therapy. *Cancer Metastasis Rev*. 2007;26:111-128.
38. O'Connor C, Wallace-Povirk A, Ning C, et al. Folate transporter dynamics and therapy with classic and tumor-targeted antifolates. *Sci Rep*. 2021;11:6389.
39. Nakai Y, Inoue K, Abe N, et al. Functional characterization of human proton-coupled folate transporter/heme carrier protein 1 heterologously expressed in mammalian cells as a folate transporter. *J Pharmacol Exp Ther*. 2007;322:469-476.
40. Menter A, Thrash B, Cherian C, et al. Intestinal transport of aminopterin enantiomers in dogs and humans with psoriasis is stereoselective: evidence for a mechanism involving the proton-coupled folate transporter. *J Pharmacol Exp Ther*. 2012;342:696-708.
41. Deng Y, Zhou X, Kugel Desmoulin S, et al. Synthesis and biological activity of a novel series of 6-substituted thieno[2,3-d]pyrimidine antifolate inhibitors of purine biosynthesis with selectivity for high affinity folate receptors over the reduced folate carrier and proton-coupled folate transporter for cellular entry. *J Med Chem*. 2009;52:2940-2951.
42. Inoue K, Nakai Y, Ueda S, et al. Functional characterization of PCFT/HCP1 as the molecular entity of the carrier-mediated intestinal folate transport system in the rat model. *Am J Physiol Gastrointest Liver Physiol*. 2008;294:G660-G668.
43. Zhao R, Visentin M, Suadicani SO, Goldman ID. Inhibition of the proton-coupled folate transporter (PCFT-SLC46A1) by bicarbonate and other anions. *Mol Pharmacol*. 2013;84:95-103.
44. Unal ES, Zhao R, Chang MH, Fiser A, Romero MF, Goldman ID. The functional roles of the His247 and His281 residues



- in folate and proton translocation mediated by the human proton-coupled folate transporter SLC46A1. *J Biol Chem.* 2009;284:17846-17857.
45. Reddy VS, Saier MH Jr. BioV Suite—a collection of programs for the study of transport protein evolution. *FEBS J.* 2012;279:2036-2046.
  46. Saier MH Jr. Eukaryotic transmembrane solute transport systems. *Int Rev Cytol.* 1999;190:61-136.
  47. Zhao R, Unal ES, Shin DS, Goldman ID. Membrane topological analysis of the proton-coupled folate transporter (PCFT-SLC46A1) by the substituted cysteine accessibility method. *Biochemistry.* 2010;49:2925-2931.
  48. Unal ES, Zhao R, Qiu A, Goldman ID. N-linked glycosylation and its impact on the electrophoretic mobility and function of the human proton-coupled folate transporter (HsPCFT). *Biochem Biophys Acta.* 2008;1778:1407-1414.
  49. Date SS, Chen CY, Chen Y, Jansen M. Experimentally optimized threading structures of the proton-coupled folate transporter. *FEBS Open Bio.* 2016;6:216-230.
  50. Duddempudi PK, Goyal R, Date SS, Jansen M. Delineating the extracellular water-accessible surface of the proton-coupled folate transporter. *PLoS One.* 2013;8:e78301.
  51. Tan J, Li X, Guo Y, et al. Hereditary folate malabsorption with a novel mutation on SLC46A1: a case report. *Medicine.* 2017;96:e8712.
  52. Diop-Bove N, Jain M, Scaglia F, Goldman ID. A novel deletion mutation in the proton-coupled folate transporter (PCFT; SLC46A1) in a Nicaraguan child with hereditary folate malabsorption. *Gene.* 2013;527:673-674.
  53. Mahadeo KM, Diop-Bove N, Ramirez SI, et al. Prevalence of a loss-of-function mutation in the proton-coupled folate transporter gene (PCFT-SLC46A1) causing hereditary folate malabsorption in Puerto Rico. *J Pediatr.* 2011;159:623-627.e1.
  54. Mahadeo K, Diop-Bove N, Shin D, et al. Properties of the Arg376 residue of the proton-coupled folate transporter (PCFT-SLC46A1) and a glutamine mutant causing hereditary folate malabsorption. *Am J Physiol Cell Physiol.* 2010;299:C1153-C1161.
  55. Atabay B, Turker M, Ozer EA, Mahadeo K, Diop-Bove N, Goldman ID. Mutation of the proton-coupled folate transporter gene (PCFT-SLC46A1) in Turkish siblings with hereditary folate malabsorption. *Pediatr Hematol Oncol.* 2010;27:614-619.
  56. Borzutzky A, Crompton B, Bergmann AK, et al. Reversible severe combined immunodeficiency phenotype secondary to a mutation of the proton-coupled folate transporter. *Clin Immunol (Orlando, FL).* 2009;133:287-294.
  57. Zhao R, Min SH, Qiu A, et al. The spectrum of mutations in the PCFT gene, coding for an intestinal folate transporter, that are the basis for hereditary folate malabsorption. *Blood.* 2007;110:1147-1152.
  58. Zhao R, Shin DS, Diop-Bove N, Ovits CG, Goldman ID. Random mutagenesis of the proton-coupled folate transporter (SLC46A1), clustering of mutations, and the bases for associated losses of function. *J Biol Chem.* 2011;286:24150-24158.
  59. Kishimoto K, Kobayashi R, Sano H, et al. Impact of folate therapy on combined immunodeficiency secondary to hereditary folate malabsorption. *Clin Immunol (Orlando, FL).* 2014;153:17-22.
  60. Erlacher M, Grünert SC, Cseh A, et al. Reversible pancytopenia and immunodeficiency in a patient with hereditary folate malabsorption. *Pediatr Blood Cancer.* 2015;62:1091-1094.
  61. Wang Q, Li X, Ding Y, Liu Y, Qin Y, Yang Y. The first Chinese case report of hereditary folate malabsorption with a novel mutation on SLC46A1. *Brain Develop.* 2015;37:163-167.
  62. Manea E, Gissen P, Pope S, Heales SJ, Batzios S. Role of intramuscular levofolate administration in the treatment of hereditary folate malabsorption: report of three cases. *JIMD Rep.* 2018;39:7-12.
  63. Min SH, Oh SY, Karp GI, Poncz M, Zhao R, Goldman ID. The clinical course and genetic defect in the PCFT gene in a 27-year-old woman with hereditary folate malabsorption. *J Pediatr.* 2008;153:435-437.
  64. Meyer E, Kurian MA, Pasha S, Trembath RC, Cole T, Maher ER. A novel PCFT gene mutation (p.Cys66LeufsX99) causing hereditary folate malabsorption. *Mol Genet Metab.* 2010;99:325-328.
  65. Shin DS, Min SH, Russell L, Zhao R, Fiser A, Goldman ID. Functional roles of aspartate residues of the proton-coupled folate transporter (PCFT-SLC46A1); a D156Y mutation causing hereditary folate malabsorption. *Blood.* 2010;116:5162-5169.
  66. Unal ES, Zhao R, Goldman ID. Role of the glutamate 185 residue in proton translocation mediated by the proton-coupled folate transporter SLC46A1. *Am J Physiol Cell Physiol.* 2009;297:C66-C74.
  67. Visentin M, Unal ES, Najmi M, Fiser A, Zhao R, Goldman ID. Identification of Tyr residues that enhance folate substrate binding and constrain oscillation of the proton-coupled folate transporter (PCFT-SLC46A1). *Am J Physiol Cell Physiol.* 2015;308:C631-C641.
  68. Najmi M, Zhao R, Fiser A, Goldman ID. Role of the tryptophan residues in proton-coupled folate transporter (PCFT-SLC46A1) function. *Am J Physiol Cell Physiol.* 2016;311:C150-C157.
  69. Zhao R, Shin DS, Fiser A, Goldman ID. Identification of a functionally critical GXXG motif and its relationship to the folate binding site of the proton-coupled folate transporter (PCFT-SLC46A1). *Am J Physiol Cell Physiol.* 2012;303:C673-C681.
  70. Wilson MR, Hou Z, Matherly LH. Substituted cysteine accessibility reveals a novel transmembrane 2–3 reentrant loop and functional role for transmembrane domain 2 in the human proton-coupled folate transporter. *J Biol Chem.* 2014;289:25287-25295.
  71. Shin DS, Zhao R, Fiser A, Goldman ID. Role of the fourth transmembrane domain in proton-coupled folate transporter function as assessed by the substituted cysteine accessibility method. *Am J Physiol Cell Physiol.* 2013;304:C1159-C1167.
  72. Aluri S, Zhao R, Fiser A, Goldman ID. Substituted-cysteine accessibility and cross-linking identify an exofacial cleft in the 7th and 8th helices of the proton-coupled folate transporter (SLC46A1). *Am J Physiol Cell Physiol.* 2018;314:C289-C296.
  73. Lasry I, Berman B, Glaser F, Jansen G, Assaraf YG. Hereditary folate malabsorption: a positively charged amino acid at position 113 of the proton-coupled folate transporter (PCFT/SLC46A1) is required for folic acid binding. *Biochem Biophys Res Commun.* 2009;386:426-431.
  74. Zhao R, Najmi M, Aluri S, Goldman ID. Impact of posttranslational modifications of engineered cysteines on the substituted cysteine accessibility method: evidence for glutathionylation. *Am J Physiol Cell Physiol.* 2017;312:C517-C526.

75. Aluri S, Zhao R, Lin K, Shin DS, Fiser A, Goldman ID. Substitutions that lock and unlock the proton-coupled folate transporter (PCFT-SLC46A1) in an inward-open conformation. *J Biol Chem*. 2019;294:7245-7258.
76. Zhan HQ, Najmi M, Lin K, et al. A proton-coupled folate transporter mutation causing hereditary folate malabsorption locks the protein in an inward-open conformation. *J Biol Chem*. 2020;295:15650-15661.
77. Wilson MR, Hou Z, Wilson LJ, Ye J, Matherly LH. Functional and mechanistic roles of the human proton-coupled folate transporter transmembrane domain 6–7 linker. *Biochem J*. 2016;473:3545-3562.
78. Yamashiro T, Yasujima T, Ohta K, Inoue K, Yuasa H. Identification of the amino acid residue responsible for the myricetin sensitivity of human proton-coupled folate transporter. *Sci Rep*. 2019;9:18105.
79. Pedersen BP, Kumar H, Waight AB, et al. Crystal structure of a eukaryotic phosphate transporter. *Nature*. 2013;496:533-536.
80. Deng D, Xu C, Sun P, et al. Crystal structure of the human glucose transporter GLUT1. *Nature*. 2014;510:121-125.
81. Deng D, Sun P, Yan C, et al. Molecular basis of ligand recognition and transport by glucose transporters. *Nature*. 2015;526:391-396.
82. Coleman JA, Green EM, Gouaux E. X-ray structures and mechanism of the human serotonin transporter. *Nature*. 2016;532:334-339.
83. Wright NJ, Lee S-Y. Structures of human ENT1 in complex with adenosine reuptake inhibitors. *Nat Struct Mol Biol*. 2019;26:599-606.
84. Abramson J, Smirnova I, Kasho V, Verner G, Kaback HR, Iwata S. Structure and mechanism of the lactose permease of *Escherichia coli*. *Science*. 2003;301:610-615.
85. Huang Y, Lemieux MJ, Song J, Auer M, Wang DN. Structure and mechanism of the glycerol-3-phosphate transporter from *Escherichia coli*. *Science*. 2003;301:616-620.
86. Yin Y, He X, Szewczyk P, Nguyen T, Chang G. Structure of the multidrug transporter EmrD from *Escherichia coli*. *Science*. 2006;312:741-744.
87. Jiang D, Zhao Y, Wang X, et al. Structure of the YajR transporter suggests a transport mechanism based on the conserved motif A. *Proc Natl Acad Sci USA*. 2013;110:14664-14669.
88. Shi Y. Common folds and transport mechanisms of secondary active transporters. *Ann Rev Biophys*. 2013;42:51-72.
89. Yan N. Structural advances for the major facilitator superfamily (MFS) transporters. *Trends Biochem Sci*. 2013;38:151-159.
90. Drew D, North RA, Nagarathinam K, Tanabe M. Structures and general transport mechanisms by the major facilitator superfamily (MFS). *Chem Rev*. 2021;121:5289-5335.
91. Wang L, Cherian C, Kugel Desmoulin S, et al. Synthesis and antitumor activity of a novel series of 6-substituted pyrrolo[2,3-d]pyrimidine thienoyl antifolate inhibitors of purine biosynthesis with selectivity for high affinity folate receptors and the proton-coupled folate transporter over the reduced folate carrier for cellular entry. *J Med Chem*. 2010;53:1306-1318.
92. Wang L, Desmoulin SK, Cherian C, et al. Synthesis, biological, and antitumor activity of a highly potent 6-substituted pyrrolo[2,3-d]pyrimidine thienoyl antifolate inhibitor with proton-coupled folate transporter and folate receptor selectivity over the reduced folate carrier that inhibits beta-glycinamide ribonucleotide formyltransferase. *J Med Chem*. 2011;54:7150-7164.
93. Bailey LB. *Folate in Health and Disease*. 2nd ed. Taylor & Francis eBooks; 2010.
94. Abramson J, Kaback HR, Iwata S. Structural comparison of lactose permease and the glycerol-3-phosphate antiporter: members of the major facilitator superfamily. *Curr Opin Struct Biol*. 2004;14:413-419.
95. Veenhoff LM, Heuberger EH, Poolman B. The lactose transport protein is a cooperative dimer with two sugar translocation pathways. *EMBO J*. 2001;20:3056-3062.
96. Dahl NK, Jiang L, Chernova MN, Stuart-Tilley AK, Shmukler BE, Alper SL. Deficient HCO<sub>3</sub><sup>-</sup> transport in an AE1 mutant with normal Cl<sup>-</sup> transport can be rescued by carbonic anhydrase II presented on an adjacent AE1 protomer. *J Biol Chem*. 2003;278:44949-44958.
97. Taylor AM, Zhu Q, Casey JR. Cysteine-directed cross-linking localizes regions of the human erythrocyte anion-exchange protein (AE1) relative to the dimeric interface. *Biochem J*. 2001;359:661-668.
98. Zottola RJ, Cloherty EK, Coderre PE, Hansen A, Hebert DN, Carruthers A. Glucose transporter function is controlled by transporter oligomeric structure. A single, intramolecular disulfide promotes GLUT1 tetramerization. *Biochemistry*. 1995;34:9734-9747.
99. Yin CC, Aldema-Ramos ML, Borges-Walmsley MI, et al. The quaternary molecular architecture of TetA, a secondary tetracycline transporter from *Escherichia coli*. *Mol Microbiol*. 2000;38:482-492.
100. Hickman RK, Levy SB. Evidence that TET protein functions as a multimer in the inner membrane of *Escherichia coli*. *J Bacteriol*. 1988;170:1715-1720.
101. Hou Z, Matherly LH. Oligomeric structure of the human reduced folate carrier: identification of homo-oligomers and dominant-negative effects on carrier expression and function. *J Biol Chem*. 2009;284:3285-3293.
102. Hou Z, Kugel Desmoulin S, Etnyre E, et al. Identification and functional impact of homo-oligomers of the human proton-coupled folate transporter. *J Biol Chem*. 2012;287:4982-4995.
103. Aduri NG, Ernst HA, Prabhala BK, et al. Human proton coupled folic acid transporter is a monodisperse oligomer in the lauryl maltose neopentyl glycol solubilized state. *Biochem Biophys Res Commun*. 2018;495:1738-1743.
104. Duddempudi PK, Nakashe P, Blanton MP, Jansen M. The monomeric state of the proton-coupled folate transporter represents the functional unit in the plasma membrane. *FEBS J*. 2013;280:2900-2915.
105. Wilson MR, Kugel S, Huang J, et al. Structural determinants of human proton-coupled folate transporter oligomerization: role of GXXXG motifs and identification of oligomeric interfaces at transmembrane domains 3 and 6. *Biochem J*. 2015;469:33-44.
106. Gupta K, Donlan JAC, Hopper JTS, et al. The role of interfacial lipids in stabilizing membrane protein oligomers. *Nature*. 2017;541:421-424.
107. Hebert DN, Carruthers A. Chololate-solubilized erythrocyte glucose transporters exist as a mixture of homodimers and homotetramers. *Biochemistry*. 1991;30:4654-4658.
108. Nomura N, Verdon G, Kang HJ, et al. Structure and mechanism of the mammalian fructose transporter GLUT5. *Nature*. 2015;526:397-401.
109. Mueller BK, Subramaniam S, Senes A. A frequent, GxxxG-mediated, transmembrane association motif is optimized for

- the formation of interhelical Calpha-H hydrogen bonds. *Proc Natl Acad Sci USA*. 2014;111:E888-E895.
110. Duan P, Wu J, You G. Mutational analysis of the role of GXXXG motif in the function of human organic anion transporter 1 (hOAT1). *Int J Biochem Mol Biol*. 2011;2:1-7.
  111. Russ WP, Engelman DM. The GxxxG motif: a framework for transmembrane helix-helix association. *J Mol Biol*. 2000;296:911-919.
  112. Polgar O, Robey RW, Morisaki K, et al. Mutational analysis of ABCG2: role of the GXXXG motif. *Biochemistry*. 2004;43:9448-9456.
  113. Gerber D, Shai Y. In vivo detection of hetero-association of glycoporphin-A and its mutants within the membrane. *J Biol Chem*. 2001;276:31229-31232.
  114. Whittington DA, Waheed A, Ulmasov B, et al. Crystal structure of the dimeric extracellular domain of human carbonic anhydrase XII, a bitopic membrane protein overexpressed in certain cancer tumor cells. *Proc Natl Acad Sci USA*. 2001;98:9545-9550.
  115. Melnyk RA, Partridge AW, Deber CM. Transmembrane domain mediated self-assembly of major coat protein subunits from Ff bacteriophage. *J Mol Biol*. 2002;315:63-72.
  116. Arselin G, Giraud MF, Dautant A, et al. The GxxxG motif of the transmembrane domain of subunit e is involved in the dimerization/oligomerization of the yeast ATP synthase complex in the mitochondrial membrane. *Eur J Biochem/FEBS*. 2003;270:1875-1884.
  117. McClain MS, Iwamoto H, Cao P, et al. Essential role of a GXXXG motif for membrane channel formation by *Helicobacter pylori* vacuolating toxin. *J Biol Chem*. 2003;278:12101-12108.
  118. Overton MC, Chinault SL, Blumer KJ. Oligomerization, biogenesis, and signaling is promoted by a glycoporphin A-like dimerization motif in transmembrane domain 1 of a yeast G protein-coupled receptor. *J Biol Chem*. 2003;278:49369-49377.
  119. Mendrola JM, Berger MB, King MC, Lemmon MA. The single transmembrane domains of ErbB receptors self-associate in cell membranes. *J Biol Chem*. 2002;277:4704-4712.
  120. Furumiya M, Inoue K, Ohta K, Hayashi Y, Yuasa H. Transcriptional regulation of PCFT by KLF4, HNF4alpha, CDX2 and C/EBPalpha: implication in its site-specific expression in the small intestine. *Biochem Biophys Res Commun*. 2013;431:158-163.
  121. Braun P, Gingras AC. History of protein-protein interactions: from egg-white to complex networks. *Proteomics*. 2012;12:1478-1498.
  122. Gonzalez MW, Kann MG. Chapter 4: protein interactions and disease. *PLoS Comput Biol*. 2012;8:e1002819.
  123. Babu M, Vlasblom J, Pu S, et al. Interaction landscape of membrane-protein complexes in *Saccharomyces cerevisiae*. *Nature*. 2012;489:585-589.
  124. Roux KJ. Marked by association: techniques for proximity-dependent labeling of proteins in eukaryotic cells. *Cell Mol Life Sci*. 2013;70:3657-3664.
  125. Roux KJ, Kim DI, Burke B, May DG. BioID: a screen for protein-protein interactions. *Curr Protoc Protein Sci*. 2018;91:19.23.1-19.23.15.
  126. Subramanian VS, Marchant JS, Said HM. Apical membrane targeting and trafficking of the human proton-coupled transporter in polarized epithelia. *Am J Physiol Cell Physiol*. 2008;294:C233-C240.
  127. Kugel Desmoulin S, Wang L, Polin L, et al. Functional loss of the reduced folate carrier enhances the antitumor activities of novel antifolates with selective uptake by the proton-coupled folate transporter. *Mol Pharmacol*. 2012;82:591-600.
  128. Chattopadhyay S, Moran RG, Goldman ID. Pemetrexed: biochemical and cellular pharmacology, mechanisms, and clinical applications. *Mol Cancer Ther*. 2007;6:404-417.

**How to cite this article:** Hou Z, Gangjee A, Matherly LH. The evolving biology of the proton-coupled folate transporter: new insights into regulation, structure, and mechanism. *FASEB J*. 2022;36:e22164. doi:[10.1096/fj.202101704R](https://doi.org/10.1096/fj.202101704R)